

# Monte Carlo Simulation of Skyrmions in 3D Lattice

Qinlian Chen, Yang Li, Ruizhong Miao, Weishuang Yin\*

January 5, 2015

## Abstract

In this paper, we followed Stefan Buhrandt and Lars Fritz's method: using classical Monte Carlo (MC) methodology to simulate the three dimensions spin structure of chiral magnets [5]. We obtained the phase diagram and depicted the real space spin texture of different phases. Then we studied the transition between the different phases and proved that choosing the initial state and the annealing methods are crucial for getting the real thermodynamics state in the simulation. At Last, we proposed a new way of manipulating skyrmions by applying a magnetic field with spacial gradient and gave the corresponding simulation result.

## 1 Introduction

Magnetic skyrmions is a kind of quasiparticles that describes a topologically protected defects in magnetic field. It has chiral spin configuration at finite temperature that is energetically stable. It was first predicted by Skyrme in 1961 [1] and has been observed experimentally either in ultra-thin magnetic film or in bulk material such as MnSi, (FeCo)Si, or FeGe [2, 3]. The most recent researches show that skyrmions on an ultra-thin film can be manipulated in a controlled way [4], which lend further support to its potential as a candidate for information storage in spintronic devices.

## 2 Model and Method

The key factor that influences the formation of skyrmions is Dzyaloshinskii-Moriya (DM) interaction, which originates from spin-orbit coupling and breaks the isotropy in a crystal. The competition of this interaction with the much stronger ferromagnetic (FM) exchange results in a twist in the magnetic order, leading to helical order. When applied a small perpendicular magnetic the phase will change to conical order. Then at some situation, the system will exhibit hexagonal symmetry as we change the temperature, this is the so-called Skyrmion phase. After taking into account the DM integration, the Hamiltonian describing chiral magnets reads:

$$H = \int \left[ \frac{J}{2a} [\nabla \mathbf{M}(\mathbf{r})]^2 - \frac{\mathbf{B} \cdot \mathbf{M}(\mathbf{r})}{a^3} + \frac{K}{a^2} \mathbf{M}(\mathbf{r}) \cdot [\nabla \times \mathbf{M}(\mathbf{r})] \right] d^3\mathbf{r}, \quad (1)$$

where  $J$ ,  $\mathbf{B}$ , and  $K$  denote ferromagnetic exchange, external magnetic field, and DM interaction, besides,  $a$  is a constant arising from the internal spin structure. For simulation purpose, the

---

\*Listed in alphabetical order of the last name

above continuum model was compactified into a discrete one:

$$H = -J \sum_{\mathbf{r}} \mathbf{S}_{\mathbf{r}} \cdot (\mathbf{S}_{\mathbf{r}+\hat{x}} + \mathbf{S}_{\mathbf{r}+\hat{y}} + \mathbf{S}_{\mathbf{r}+\hat{z}}) - B \cdot \sum_{\mathbf{r}} \mathbf{S}_{\mathbf{r}} - K \sum_{\mathbf{r}} (\mathbf{S}_{\mathbf{r}} \times \mathbf{S}_{\mathbf{r}+\hat{x}} \cdot \hat{x} + \mathbf{S}_{\mathbf{r}} \times \mathbf{S}_{\mathbf{r}+\hat{y}} \cdot \hat{y} + \mathbf{S}_{\mathbf{r}} \times \mathbf{S}_{\mathbf{r}+\hat{z}} \cdot \hat{z}), \quad (2)$$

where  $\hat{x}$ ,  $\hat{y}$ , and  $\hat{z}$  are the basis vectors of the simple cubic lattice. The ratio of  $J/K$  determines the diameter of skyrmion helices at a constant temperature and field. We choose that  $J = 1$  and  $K = \tan(2\pi/10)$ . The next-nearest neighbor interactions are also considered for better approximation, which has the form:

$$H' = J' \sum_{\mathbf{r}} \mathbf{S}_{\mathbf{r}} \cdot (\mathbf{S}_{\mathbf{r}+2\hat{x}} + \mathbf{S}_{\mathbf{r}+2\hat{y}} + \mathbf{S}_{\mathbf{r}+2\hat{z}}) + K' \sum_{\mathbf{r}} (\mathbf{S}_{\mathbf{r}} \times \mathbf{S}_{\mathbf{r}+2\hat{x}} \cdot \hat{x} + \mathbf{S}_{\mathbf{r}} \times \mathbf{S}_{\mathbf{r}+2\hat{y}} \cdot \hat{y} + \mathbf{S}_{\mathbf{r}} \times \mathbf{S}_{\mathbf{r}+2\hat{z}} \cdot \hat{z}), \quad (3)$$

The values of  $J'$  and  $K'$  are  $J' = J/16$  and  $K' = K/8$ . The simulation was conducted on a  $30 \times 30 \times 30$  simple cubic lattice, and the periodic boundary condition was used. The controllable parameters are  $T$  (temperature) and  $B$  (external field). Other parameters keep fixed throughout the simulation.

## 3 Result

### 3.1 Global Phase Diagram

Our first task focuses on the phase diagram of the model. We use the local chirality, which corresponds to the density of skyrmions, to identify the skyrmion phase. The mathematical expression of chirality reads:

$$\chi_{\mathbf{r}} = \frac{1}{8\pi} \epsilon_{ij} \mathbf{S}_{\mathbf{r}} \cdot (\mathbf{S}_{\mathbf{r}+\hat{i}} \times \mathbf{S}_{\mathbf{r}+\hat{j}}), \quad (4)$$

where  $\epsilon_{ij}$  is antisymmetric tensor and Einstein summation convention is used. In our simulation, we found that the two dimensional chirality is sufficient to distinguish skyrmion phase from other phases, while the result given by the three dimensional chirality doesn't differ too much from it. This is due to the tube-like spin configuration, in which the skyrmions propagate along the direction of the external field.

Another issue we have to deal with is that this spin model is very hysteretic, which means different initial states and different annealing methods can lead to different final states, and the system is often trapped into a metastable state. To address this, three different annealing methods were implemented, namely, (i) cooling at a constant field, (ii) cooling to the target temperature at zero field followed by slowly increasing the field. (iii) cooling to the target temperature at a high field (such that we always remain in the spin-polarized phase) followed by decreasing the field. These three annealing methods were conducted in parallel, and the one with the lowest energy was considered to be the real thermodynamic state. In the initial state, all spins point against the direction of the external field (The completely random initial state is also tried and yields the similar result). Under this scheme, we are able to give the global phase diagram of a skyrmion lattice (Figure.1).

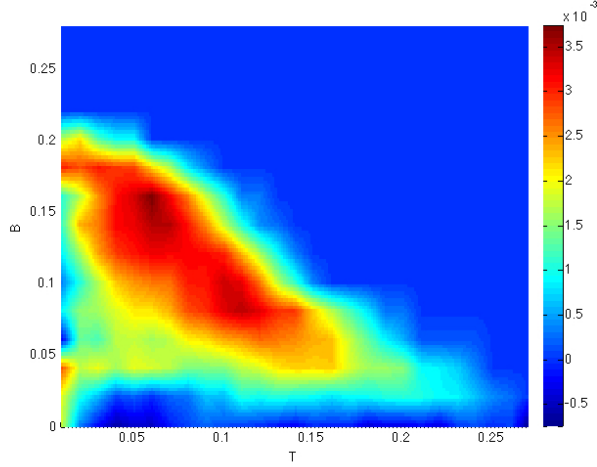


Figure 1: Global phase diagram. Red color indicates high skyrmion density.

From the phase diagram, we can find the region at intermediate magnetic field and temperature slightly above zero in which the skyrmion phase is stable. It can also be observed from this figure that although the same indicator of skyrmion, 2D chirality, is used, the phase diagram of 3D skyrmions is different from its 2D counterpart. In order to have a direct vision, the real space spin textures in different phases were plotted in Figure 2.

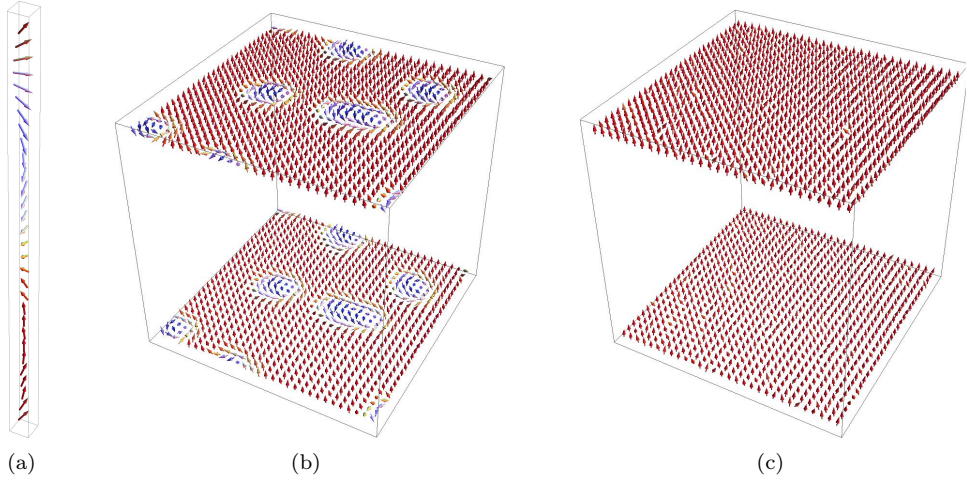


Figure 2: Real space spin textures of (a) helical phase ( $T = 0.03, B = 0.02$ ), (b) skyrmion phase ( $T = 0.09, B = 0.12$ ), and (c) paramagnetic phase ( $T = 0.20, B = 0.16$ ).

### 3.2 Thermodynamics across Temperature-Driven Phase Transition

After obtaining the global phase diagram, we proceed to investigate the thermodynamic quantities of the system. In order to observe phase transitions from skyrmion to other phases, we fix  $B = 0.1$  so that the system crosses the skyrmion phase region, which is indicated by the phase

diagram in Figure 1. As has been said in the previous section, the system in simulation suffers from hysteresis, thus the real thermodynamic state of different temperature cannot be simulated in a row, on which point we will give further analysis in next section. We here first use the three annealing methods same as mentioned above, and choose the one with the lowest energy. Meanwhile, before the simulations under each temperature, the initial state is reset to the one that all spins points against the direction of external field. We do so to make sure that data points are independent of each other and hysteretic effect is thus avoided. Our results obtained under this scheme is presented in Figure 3.

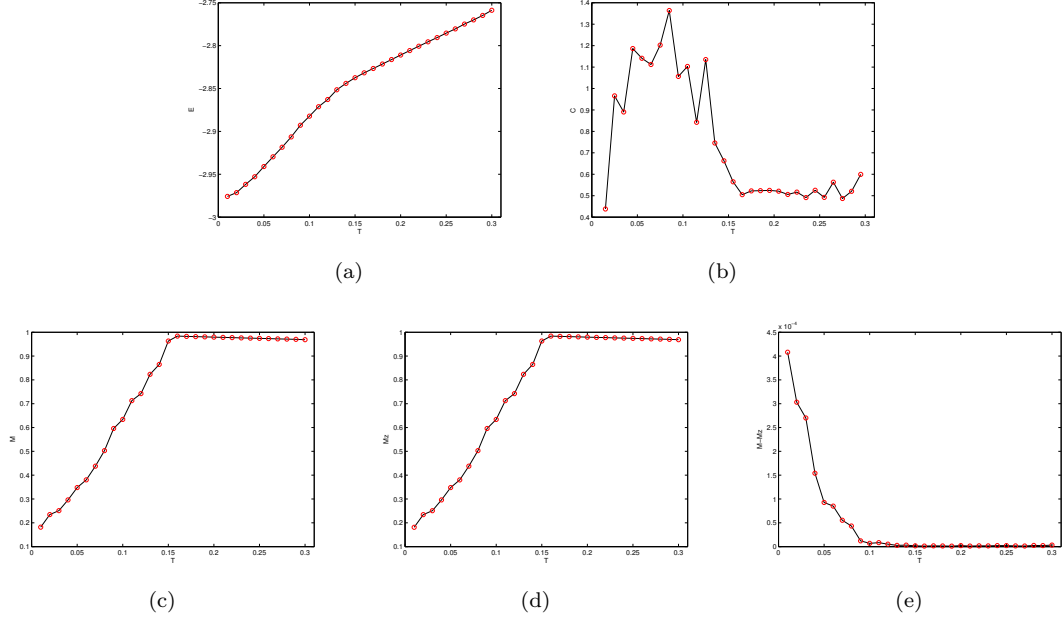


Figure 3: Plots of thermodynamic quantities under different temperature: (a) Energy per site ( $E$ ) vs Temperature ( $T$ ); (b) Specific heat ( $C$ ) vs Temperature ( $T$ ); (c) Magnetization ( $M$ ) vs Temperature ( $T$ ); (d) Magnetization along z-axis ( $M_z$ ) vs Temperature ( $T$ ); (e) Difference of  $M$  and  $M_z$  vs Temperature ( $T$ ).

From the above figure, it can be seen that there is an obvious phase transition whose critical temperature is  $T = 0.15$ . this corresponds to the phase transition between skyrmion phase and paramagnetic phase. When  $T < 0.15$ , the stable helical order of skyrmions keeps the system from reaching paramagnetic state. As  $T$  goes beyond 0.15, this helical order is broken by the thermal fluctuation and the spins follows the direction of the external field. As a result, the magnetization reaches the neighborhood of 1. It can also be seen from Figure 3(b) that the critical temperature can also be revealed by  $T - C$  plot and the specific heat at low temperature is relatively higher than that at higher temperature.

The overall magnetization  $M$  and the Magnetization along z-axis  $M_z$  are almost same to each other. This is due to the effect of the external field: the overall magnetization is almost all contributed by its z-axis component. Interestingly, we plot the difference of  $M$  and  $M_z$  against temperature and observe a seeming phase transition at  $T = 0.1$ , which means above this temperature, the contribution of horizontal magnetization to the overall  $M$  disappears.

It is also worth noting that there is no obvious indication of phase transition between conical

and skyrmion phases from the above thermodynamic quantities. To distinguish these two phases, the method of using chirality is still the first choice.

### 3.3 Analysis of Initial States

Considering the hysteresis of the model. We tried three different schemes of annealing, and different final states can often be observed despite that they share the same initial state. The three schemes were:

- (1) raising temperature at zero field followed by increasing the field to the target intensity
- (2) raising temperature at high field followed by decreasing the field to the target intensity
- (3) dropping temperature at non-zero constant field

Because the paramagnetic state are favored at high temperatures or at high field, scheme (2) and (3) are prone to be trapped in paramagnetic state from the beginning and therefore no skyrmions were observed under these two schemes.

Regarding scheme (1), final state varied when the initial state was manipulated differently. When all spins were set to  $z$  direction at the beginning, the final state was paramagnetic. In contrast, skyrmions appear when each spin was manipulated in a certain way at the beginning.

We tried different initial states to see its influence to the final state. It turned out that skyrmions would grow from the spin down part (blue), as is shown in Figure 4.

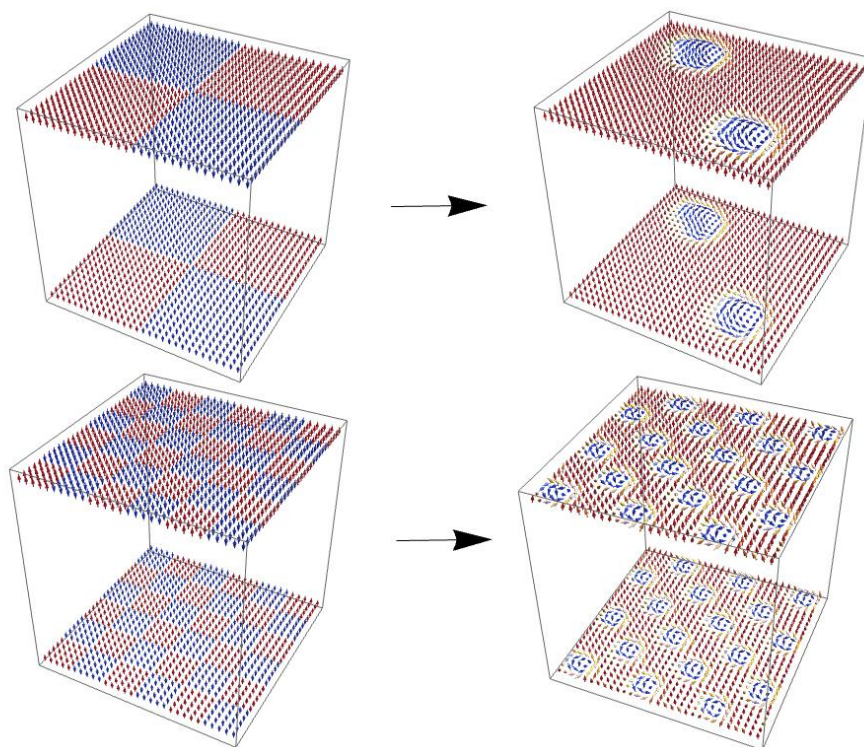


Figure 4: The corresponding final states to different initial states

Using the manipulated initial state, we try to simulate temperature-driven phase transition by increasing the temperature in a row. The configuration of initial state at the bottom-left of Figure 4 was chosen and the temperature was changed from 0.01 to 0.20 with step 0.01 at different field(0.05 and 0.10). At  $B = 0.1$ , the  $E - t$  and  $M_z - t$  relation are shown in Figure 5. Notably, they were simulated in a row, which is in contrast to the previous section:  $T = 0.01$  was simulated first followed by  $T = 0.02$  and so forth. In other word,  $T = 0.01$  can be deemed as the initial state of  $T = 0.02$ . Under this method, a first order phase transition and a second order one occur at  $T = 0.15$  and  $T = 0.10$  respectively. However, the initial state was manipulated and annealing method is lacked, two phase transitions may result from this. Comparing this result with the ones in the previous section, we can conclude that the initial state can affect the fundamental characteristics of the final state and therefore must be taken seriously.

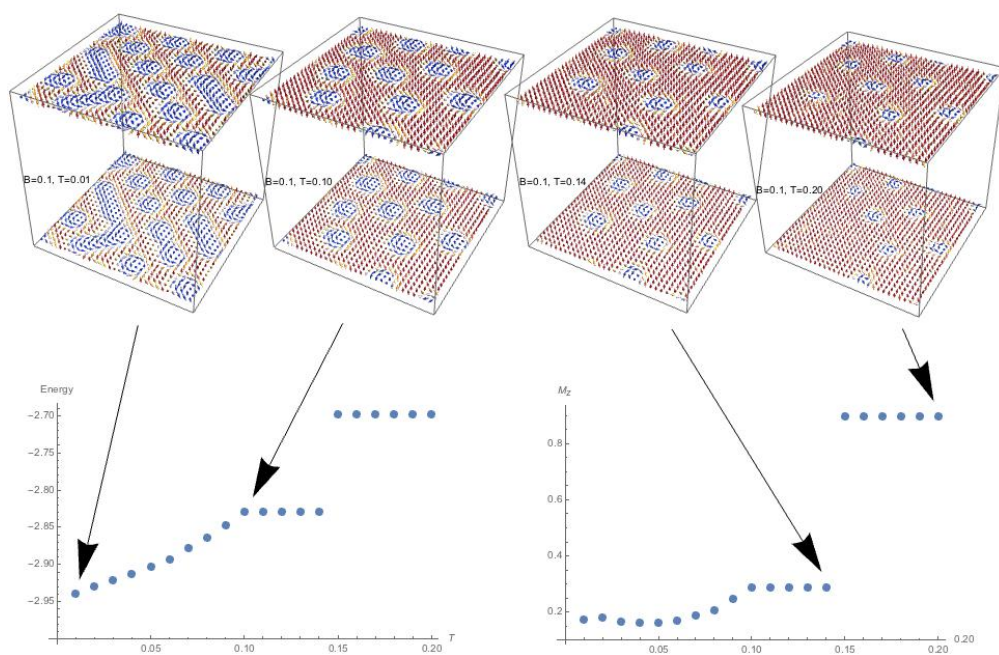


Figure 5:  $B = 0.1$

Starting with a random initial state, we raise the temperature from 0.005 to 0.25 and record the average  $E$  and  $M_z$  every 0.005. This process is repeated with different random initial state. Thus, for each temperature, we have several  $\{E, M_z\}$  pairs and only the one with the smallest  $E$  are chosen. As is Shown in Figure 6(c), we can see the result similar to the previous section is partially recovered. Other differences at high temperature between Figure 6 and Figure 3 can be explained by different annealing methods. This result shows the influence of initial state is not negligible and suggests the necessity of PTMC.



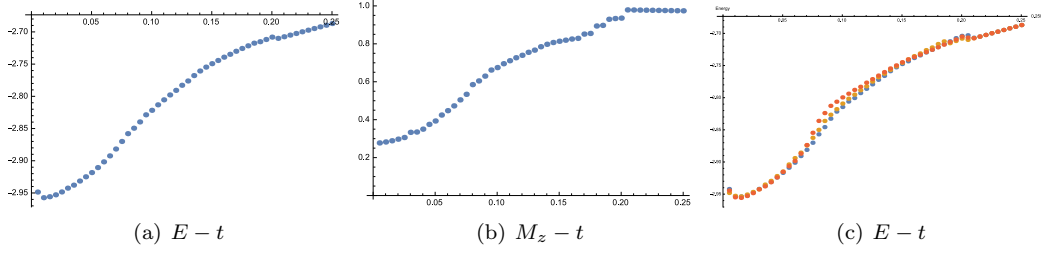


Figure 6: (c) shows the  $E$ - $t$  relation of different initial state. Selecting the  $\{E, M_z\}$  with smallest  $E$ , we got (a) and (b).

### 3.4 Manipulation of Skyrmion

Since skyrmion is a promising storage unit, we try to find a possible way to control it via Monte Carlo simulation thus illuminating practical implementation. As is shown in the phase diagram, skyrmions are favored at  $B = 0.1$  while not at  $B = 0.4$ . Therefore, a magnetic field window is applied to the system (Figure 7) in order to simulate magnetic field with spatial gradient. In our simulation, the magnetic field window starts at the position in Figure 7(a) and end as in Figure 7(c). The window moves one spin right every 10000 MC steps. It is found that the skyrmion inside the magnetic field window is confined and moves together with it.

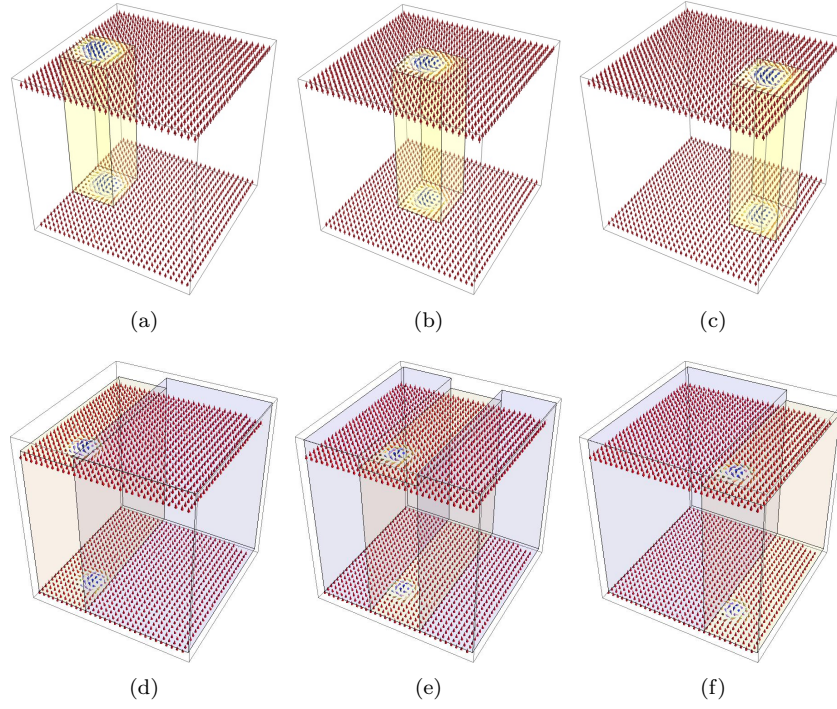


Figure 7: From (a) through (c): a magnetic field window moves from left to right. From (d) through (f): a magnetic field ravine moves from left to right. In both cases, the skyrmion is confined inside and driven to move with the well. The magnetic field window is shown as the yellow cuboid.  $B = 0.1$  inside and  $B = 0.4$  outside.

Apart from the magnetic field window, we have also tried other shapes of magnetic field well, for example a magnetic ravine, and similar results can be obtained. These results suggest the possibility of controlling skyrmions by manipulating the magnetic field.

## 4 Conclusion and Discussion

Through Monte Carlo simulation we reproduced the phase diagram of skyrmion lattice model at finite temperature and external magnetic field. It is confirmed that the skyrmion phase need to be stabilized by a certain amount of thermal fluctuation and magnetic field. This is in contrast to the phase diagram of 2D cases. The basic thermodynamic quantities are investigated to study their temperature-driven phase transitions. We also analyzed the effects of different initial states on the final states observed, and concluded that the final state in the simulation depends heavily on their initial states, thus it is necessary to conduct simulation with different initial states and annealing methods. In the end, as a predicting simulation, we apply a magnetic field with spacial gradient to the system and successfully change the position of a skyrmion by moving the external field. This shows a promising way of manipulating skyrmions in laboratory and is worth further investigation.

## References

- [1] T.H.R. Skyrme, *A non-linear field theory*, 1961 *Proc. R. Soc. Lond. A* **260**
- [2] S. Muhlbauer, B. Binz, F. Jonietz, C. Pfleiderer, A. Rosch, A. Neubauer, R. Georgii, and P. Boni, *Skyrmion lattice in a chiral magnet*, 2009 *Science* **323**
- [3] X. Z. Yu, Y. Onose, N. Kanazawa, J. H. Park, J. H. Han, Y. Matsui, N. Nagaosa and Y. Tokura, *Real-space observation of a two-dimensional skyrmion crystal*, 2010 *Nature* **465**
- [4] Stefan Heinze, Kirsten von Bergmann, Matthias Menzel, Jens Brede, Andr Kubetzka, Roland Wiesendanger, Gustav Bihlmayer and Stefan Blgel, *Spontaneous atomic-scale magnetic skyrmion lattice in two dimensions*, 2011 *Nature Physics* **7**
- [5] Buhrandt, S. and L. Fritz, *Skyrmion lattice phase in three-dimensional chiral magnets from Monte Carlo simulations*, 2013 *Physical Review B* **88**



## Contributions

苗睿中：完成skyrmion点阵的编程和部分模拟，找到skyrmion相的参数，完成了论文中“Global Phase Diagram”和“Thermodynamics across Temperature-Driven Phase Transition”部分的研究和相应部分论文撰写，部分“Introduction”的撰写。同时作为队长，负责协调各个组员的工作和汇总信息。

李阳：完成skyrmion点阵的编程和部分模拟，使用mathematica完成三维skyrmion自旋图和动态图的程序，完成了论文中“Analysis of Initial States”和“Manipulation of Skyrmion”部分的研究和相应部分论文撰写，部分“Thermodynamics across Temperature-Driven Phase Transition”方面的研究。

尹卫爽：部分skyrmion点阵的编程，代码运行，部分画图工作，论文中部分“Introduction”的写作，部分“Manipulation of Skyrmion”的研究和相应部分论文撰写。

陈沁连：代码维护和运行，部分数据处理。